Tire Parameters for Landing-Gear Shimmy Studies

R. L. COLLINS* AND R. J. BLACK†
The Bendix Corporation, South Bend, Ind.

This paper discusses a tire-test machine, similar to a free-castering landing gear, which allows the determination of tire parameters necessary for accurate prediction of shimmy stability of landing gears. An adequate set of tire parameters is shown to be k_1, lateral tire-spring rate; C_L, lateral viscous-damping coefficient; C, coefficient of yaw; C_1, yaw time constant; and μ_1, tire torsional spring constant. k_1 and C_L are determined from standing tire-deflection and die-away tests. The rolling tire-test machine is used to determine values for C, C_1, and μ under simulated high-speed and low-speed taxi runs. Results for two different tires are given (18×5.5, 14-ply and 49×17, 26-ply). The importance of accurate tire data is demonstrated by showing how stability maps of a typical landing gear vary with changes in tire parameters.

Nomenclature

A	= absolute value of amplitude ratio of consecutive peaks
C	= tire-yaw coefficient, rad/lb
C_1	= tire-time constant, sec/rad
C_H	= hydraulic damping coefficient, in.-lb-sec²/rad²
e	= error function of experimental and theoretical amplitude ratios
f_s	= shimmy frequency, cps
F_t	= side force on wheel due to tire deformation, lb
F_z	= vertical force on wheel, lb
I	= inertia about pivot, lb-sec²-in.
I_0,I_1,I_2	= experimentally determined coefficients, lb-sec²-in., lb-sec², lb-sec²/in., respectively
k_1	= lateral tire stiffness, lb/in.
C_L	= lateral tire damping, lb-sec/in.
L	= trail length, in.
L_p	= pneumatic trail length, in.
M_A	= moment applied to test rig, in.-lb
M_B	= moment due to bearing friction, in.-lb
M_t	= moment on wheel due to tire deformation, in.-lb
Δ	= lateral deformation of tire, in.
μ_{D1},μ_1,μ_s	= tire-torsional coefficients, in.-lb/rad
ψ	= yaw angle of wheel, rad
ψ_t	= yaw angle of tire footprint, rad

I. Introduction

EVER-INCREASING emphasis on reducing the weight of landing-gear systems in modern aircraft has, in many cases, led to landing-gear shimmy problems. The shimmy problem has been encountered in nose and tail landing-gear systems for some time and more recently has been observed in main landing gears. Analysis for the prediction of instability is an important part of landing-gear design and also serves as a guide in shimmy testing programs.

Two basic analytical techniques have been suggested for determining the forces on a wheel due to tire deflections: the theory of Von Schlippe[1] and the hypothesis of Moreland.[2] The constitutive relations of either method require the knowledge of certain coefficients or parameters which are a function of the properties of the particular tire under consideration. Often only limited success is achieved in shimmy analyses mainly because of insufficient experimental (or theoretical) data on these parameters. Smiley and Horne[3] have presented an excellent survey of available data up to 1960 on various tire parameters, but some important parameters are not found even here. Smiley and Horne's report shows that there may be considerable difference in the values of the parameters depending upon the tire design as well as size. Another limitation of past data is that most data on rolling tires were taken at low rolling speeds (3 or 4 mph) thus reducing its reliability for studies at normal taxi, takeoff, and landing speeds.

Received March 22, 1968; also presented as Paper 68-311 at the AIAA/ASME 9th Structures, Structural Dynamics, and Materials Conference, Palm Springs, Calif., April 1–3, 1968; revision received September 19, 1968. The authors wish to gratefully acknowledge the assistance and support of the Lockheed-Georgia Company.

*Senior Analyst, Analytical Mechanics Department, Energy Controls Division.

†Supervisor, Dynamics Analysis Group, Analytical Mechanics Department, Energy Controls Division.

II. Analytical Background

A landing-gear system may be analyzed as a lumped mass frame which has a shimmy damper, usually an integral part of the steering mechanism, and which is being acted upon by an "external" force system due to the tire-ground reaction. A schematic of such a system is presented in Fig. 1. The general form of the inertial equations for the system is

$$\sum_{j=1}^{N} m_{ij}\ddot{q} + \sum_{j=1}^{N} C_{ij}\dot{q}_j + \sum_{j=1}^{N} k_{ij}q_j = Q_i \qquad (1)$$

$$i = 1, 2, \ldots, N$$

where m_{ij} is the generalized inertia matrix, C_{ij} the equivalent viscous damping matrix for the structure, k_{ij} the stiffness matrix of the structure, and q_i the N generalized coordinates of the structure. The Q_i are the generalized forces which in general are not derivable from a potential function but are dependent upon other system coordinates not included in the q_i. The Q_i functions include such quantities as nonlinear strut torsional forces and moments. The nonlinearities arise from mechanical play of the torque arm linkages, hydraulic and friction damping in the shimmy damper unit, and the important external force due to tire deformations. Although these generalized forces can be nonlinear and nonconservative, they are well-defined functional relationships. The unknown quantities are the tire force F_t and the tire moments M_t acting on each wheel.

It has been mentioned that there are two basic developments in tire mechanics for the representation of the forces acting on a wheel due to tire deformations. The theory of Von Schlippe relates these forces to a finite tire-footprint length by a set of differential and algebraic equations which are rather unwieldy, although solvable. The second method is derived from the suggestion by Moreland which relates the force acting on the wheel to the tire-distortion angle ψ_t and its derivative $\dot{\psi}_t$. Moreland's equation is used in this study as

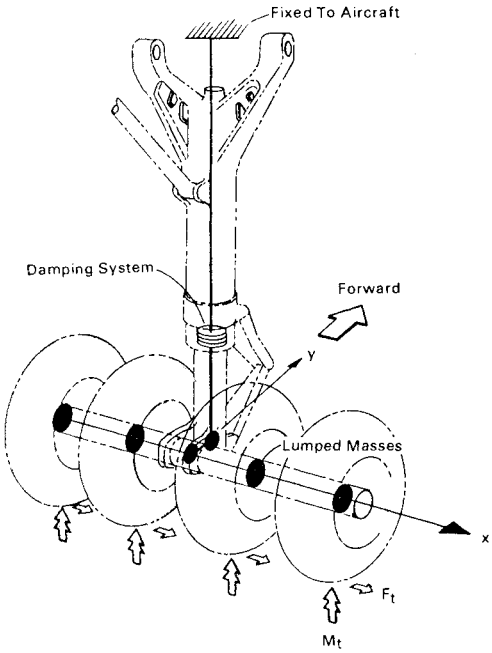

Fig. 1 Lumped mass frame representing typical multi-wheel landing-gear system.

it is simpler than von Schlippe's and yet provides excellent correlation with experimental data in both the present study and in past studies, such as that of Ref. 4.

The tire distortion is defined by two variables: the lateral deflection of footprint center Δ, and the torsional twist of the footprint relative to the wheel plane ψ_t. These coordinates are shown in Fig. 2. The distortions of the tire are, of course, due to ground forces acting on the footprint, and these ground forces (and moments) are transmitted through the tire to the wheel. The force system transmitted through the distorted tire is reduced to an equipollent system at the lowermost portion of the wheel in the wheel plane. This reduced force system has the tire force F_t acting normal to the wheel plane, the horizontal drag force F_D in the wheel plane, the vertical ground reaction F_z, and the moment M_t.

The force F_t is assumed to be related to the deflection Δ and its derivative $\dot{\Delta}$ as an ordinary spring-damper system, so that

$$F_t = k_1\Delta + C_L\dot{\Delta} \tag{2}$$

where k_1 is the effective lateral stiffness and C_L is the effective lateral damping of the tire. Moreland's hypothesis states that this "side force" F_t is also related to the tire yaw angle ψ_t during rolling, as

$$CF_t = \psi_t + C_1\dot{\psi}_t \tag{3}$$

where C is referred to as the tire-yaw coefficient and C_1 as the tire-time constant.

The moment due to tire twisting and footprint distortion under rolling conditions is a highly complicated physical occurrence, especially when one considers that a tire is probably quite nonlinear in its deformation due to the several fibrous inner layers. This twisting moment depends to a large extent on the tread design and tire geometry as well as on these inner layers. In any case, it might reasonably be expected that the moment M_t be represented as a function of the twist angle ψ_t in the form

$$M_t = \mu_s\psi_t + \mu_{D1}\dot{\psi}_t + \mu_2\psi_t^2 + \ldots \tag{4}$$

where μ_s represents the static torsional spring coefficient and μ_{D1}, μ_2 are the coefficients of the series representing the additional effects under tire rolling conditions. For this paper the coefficients of the higher-order terms will be assumed small

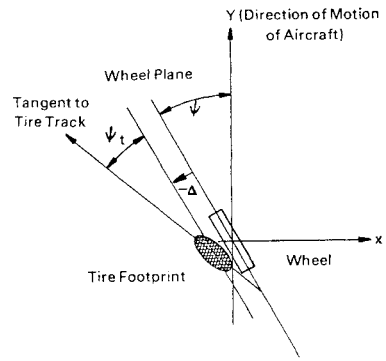

Fig. 2 Tire deformation variables Δ and ψ_t.

enough that

$$M_t = \mu_1\psi_t \tag{5a}$$

where,

$$\mu_1 = \mu_s + \mu_{D1} \tag{5b}$$

Each wheel in the system will have a set of equations, such as 2, 3, and 5, which describe the system excitation forces. In addition to Eqs. (1–3 and 5) the constraint of rolling without slipping, along the tire track, must be met by the footprint center contact point. This constraint leads to another differential equation for each tire, and these give a complete set of differential equations from which the system stability may be determined.

A tire-test machine was designed to obtain data at high, as well as low, rolling speeds. A schematic of the tire-test rig is shown in Fig. 3. This test machine is used to measure three of the tire parameters: C, μ_1, and C_1. It is essentially a castered wheel, fixed to oscillate at some trail distance L from the wheel center and mounted above a rotating drum. The tire is pressed onto this drum with a measured vertical force F_z, while the rotating drum simulates a runway velocity V.

The equations of motion of the rolling tire-test machine are simplifications of Eqs. (1–5). The summation of moments about the pivot shows that

$$M_A + LF_t + M_t + M_B = I\ddot{\psi} \tag{6}$$

where M_A is the applied moment about the pivot and M_B denotes the frictional losses in the machine bearings. This equation along with (2, 3, and 5) and the kinematic rolling constraint are used in the determination of the tire parameters as shown in the following sections of this paper. In Eq. (6), the moment of inertia of the test machine, wheel and tire system I, will vary with the trail length L as

$$I = I_0 - I_1L + I_2L^2 \tag{7}$$

This relationship occurs since the axle position remains above

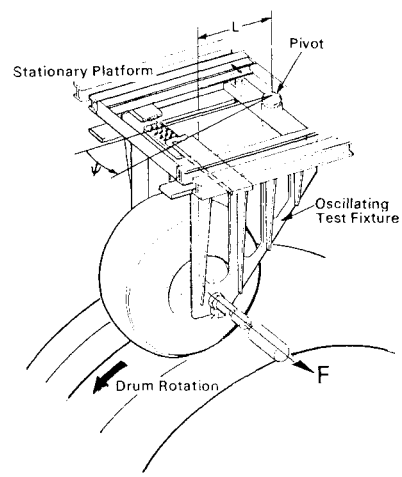

Fig. 3 Illustration of rolling tire-test rig.

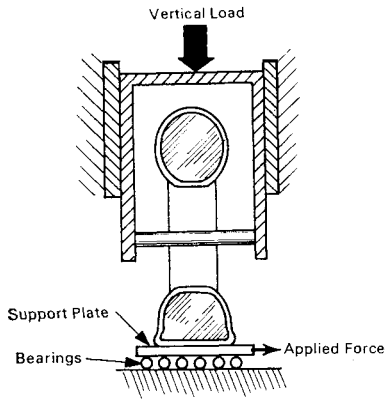

Fig. 4 Schematic of static test fixture.

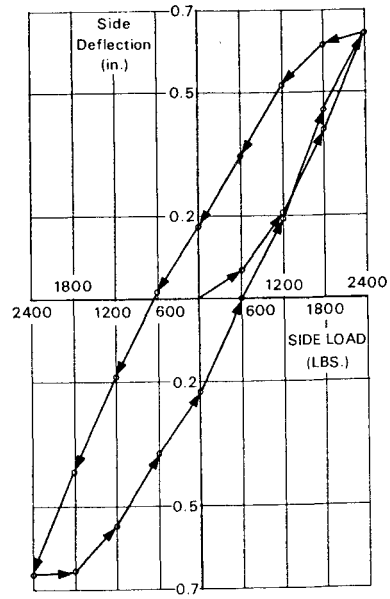

Fig. 5 Example of tire data for lateral stiffness— 49 x 17, 26 PR, Type VII tire; F_z = 6000 lb, p = 130 psi.

the rolling drum centerline while the pivot position is moved fore and aft in order to vary the trail length L.

III. Tire Parameter Determination

Standing Tire Tests

Tests were performed with a standing or nonrolling tire for the determination of the lateral stiffness k_1, the lateral effective damping C_L, and the static torsional stiffness μ_s. The tests were made in a static test fixture with a movable supporting plate as shown schematically in Fig. 4.

Lateral stiffness

The lateral stiffness of an 18 × 5.5, 14-ply rating, type VII tire and a 49 × 17, 26-ply rating, type VII tire were determined under the conditions shown in Table 1. The stiffness was obtained by applying a measured lateral force to the supporting plate, which rests on ball bearings, and measuring the resulting deflection of the plate. Tires exhibit very nonlinear deformation characteristics and the lateral force-deflection curves for both tires show a large hysteresis loop. A typical plot of this data is shown in Fig. 5. This data were taken over an extended period of time so that frequency of the loop travel does not contribute to the energy dissipated per cycle. Therefore, the assumption of Eq. (2) is unrealistic from consideration of this energy dissipation as the actual work done per cycle is due more to friction and deformation of the internal fibers than to the rate of motion.

Equation (2) appears sufficient for the purposes of present stability analyses. However, it is very likely that a more refined analysis considering the static hysteresis effect would be of value in future stability studies. Correlation of the experimental shimmy data presented in Sec. IV of this paper indicates that the tire-yaw shimmy mode obtained was not strongly dependent on the parameter k_1; however, the structural torsion shimmy mode is considerably more sensitive to this value. The values of k_1 were obtained by fitting a straight line ($y = mx + b$) through the hysteresis loops with a least-square error criteria.

Table 1 Measured values of tire parameters

Tire	F_z	P psi	k_1 - lb./in.		C_L-lb.-sec./in.		μ_1 - in.-lb./rad.	
			Nom.	Range+	Nom.	Range+	Nom.	Range
18 x 5.5	775	78	1830	.7-1.5	12.0	0-1.0	0	$\pm 2\times10^{4}$
18 x 5.5	775	105	1865	.85-1.3	12.6	0-1.0	0	$\pm 1.8\times10^{4}$
18 x 5.5	3100	78	1335	.8-1.3	8.8	0-1.0	0	$\pm 5.4\times10^{4}$
18 x 5.5	3100	105	1615	.9-1.2	8.9	0-1.0	0	$\pm 5.1\times10^{4}$
49 x 17	6000	130	3420	.9-1.7	46.9	0-1.0	0	$\pm 27\times10^{4}$
49 x 17	25000	130	4060	.9-1.3	28.8	0-1.0	0	$\pm 97\times10^{4}$

Tire	F_z	P psi	Steady State C - rad./lb.		Free Oscillation C - rad./lb.		C_1 - sec.	
			Nom.	Range+	Nom.	Range+	a_1*	b_1*
18 x 5.5	775	105	1.34×10^{-4}	.6-1.3	1.53×10^{-4}	.95-1.06	$.04\times10^{-4}$	2×10^{-4}
18 x 5.5	3100	105	$.75\times10^{-4}$	.7-1.13	$.75\times10^{-4}$	.8 -1.2	$.011\times10^{-4}$	0
49 x 17	6000	130	$.36\times10^{-4}$	.67-1.28	$.23\times10^{-4}$	.85-1.01	$.002\times10^{-4}$	0
49 x 17	25000	130	$.141\times10^{-4}$	.33-1.27	$.07\times10^{-4}$	.75-1.29	0	1×10^{-4}
49 x 17	37500	130	$.048\times10^{-4}$	.4-1.4	$.08\times10^{-4}$	.9 -1.06	0	1×10^{-4}

+Values are ratios to nominal

*a_1, b_1 are constants such that $C_1 = a_1V + b_1$ where: V(in./sec.)

Static torsional stiffness

The static torsional stiffness μ_s was determined by applying a moment to the support plate of the static test rig and measuring the resulting plate angular deflection. The hysteresis loops obtained in this case were very large and, as pointed out in Ref. 3, depend on the amplitude of the deflection. The resulting value of μ_s was obtained by a least-squares fit of a straight line, as in the case of lateral stiffness. Since the torsional moment of the tire during rolling is found to be considerably less than the static moment, further discussion of this value is found in the section on rolling tire tests.

Lateral effective damping coefficients

In order to account for energy losses of the test tires during deformations, a simple linear velocity damper was assumed acting on the lateral tire-deflection coordinate Δ as shown in Eq. (2). Although such a mechanism does not properly account for energy dissipation at very low frequencies, the approximation appears to be sufficient for the normal shimmy frequencies of 3–15 cps. In order to obtain an estimate of the effective damping, the supporting plate of Fig. 5 was pulled to one side and released. The ensuing motion of the support plate was recorded, and from the measured amplitude decay and oscillation frequency the effective damping and lateral spring constant were computed. The results of these tests are given in Table 1. The free oscillation frequencies are also tabulated. The masses of the support plates were 0.48 lb-sec^2/in. for the 18 × 5.5 tire and 1.88 lb-sec^2/in. for the 49 × 17 tire. The actual energy-dissipation mechanism during rolling will of course be different from that of the lateral deformation so that the C_L values should be used solely as guides during an analysis of shimmy. From experience gained through recent analyses, it is recommended that the values of C_L given in Table 1 be used as upper limits of the amount of damping which might be expected during rolling conditions.

Rolling Tire Tests

The values shown in Table 1 for the tire-yaw coefficient C, the torsional stiffness μ_1, and the tire-time constant C_1 were obtained from data taken from the rigid, pivotable test machine shown in Fig. 3.

Steady-state yaw coefficient

The tire-yaw coefficient was obtained under both steady-state and oscillating, rolling conditions. The tire is pressed onto a revolving steel drum at a known vertical force F_z and drum surface speed V. A lateral force is applied at the axle, rotating the tire and test rig about the test rig pivot through a measured angle ψ. The tire footprint then must twist to the angle ψ_t where, by sign convention, $\psi_t = -\psi$.

After steady state is reached the forces and moments acting about the test rig pivot must satisfy the equilibrium equation,

$$LF_t + M_t = -M_A - M_B$$

and under the assumptions of Eqs. (3) and (5a) thee xpression becomes

$$(1/C) + (1/L)\,\mu_1 = -(1/\psi_t)(M_A/L + M_B/L) \qquad (8)$$

it should be noted from Eq. (8) that the reactions at the pivot (excluding friction) do not appear in this relation, which is an advantage of testing at a nonzero trail length L. The bearing friction moment M_B was assumed negligible for the steady-state tests.

At a given speed V and loading F_z, a series of measurements of the applied moment M_A and the angle ψ_t were made for several values of L. As C and μ_1 are not dependent upon ψ_t, the right-hand side of Eq. (8) will ideally give the same value for each (M_A, ψ_t) measurement. Since there is some degree of data scatter, the values for the right-hand side of Eq. (8) are averaged over all the (M_A, ψ_t) measurements for each trail length L. If this averaged value is called $\tilde{L}$ then Eq. (8) becomes

$$(1/C) + (1/L_i)\,\mu_1 = \tilde{L}(L_i) : i = 1, 2, \ldots, N \qquad (9)$$

Now C and μ_1 are also (ideally) independent of the trail length as they are properties of the tire, and therefore, if N trail lengths are considered, Eq. (9) may be used to solve for C and μ_1. A least-square error procedure was used for finding C and μ_1 which best fit Eq. (9).

These values obtained were used to develop Table 1. The values of trail lengths used were: 18 × 5.5 tire, L = 4, 8, 12, 20, 24, 30 in.; 49 × 17 tire, L = 24, 28, 30, 34, 38, 42 in., although not all of the trail lengths were used during any one of the 49 × 17 tire-test conditions.

It was found that the value of μ_1 was too small to be accurately measured with this test technique. However, the values of μ_1 determined from the least-squares fit of the data were within the data scatter band, and from the reduced data it was concluded that the maximum value of μ_1 is within a range of ±100% of its static value μ_s. There are several reasons for the difficulty in obtaining the torsional moment in this manner, not the least of which is the large amount of natural or static hysteresis which requires a more elaborate expression for the torsional moment than that given by Eq. (4). The revolving-drum curvature leads to errors since this affects the pressure center of the tire footprint and varies with both ψ_t and L, thereby causing both C and μ_1 to be functions of ψ_t and L. Also there is the very likely possibility of an erratic slippage of the outer portions of the tire footprint while rolling during the twisted condition.

If one assumes that the rolling torsional tire stiffness is negligible, a value of C may be determined directly from Eq. (9) for each L. The average of the yaw coefficient for all the trail lengths tested with μ_1 assumed to be zero is included in the suggested ranges given in Table 1.

The data indicated that C is essentially independent of the rolling speed so that the values shown in Table 1 are averaged from the several test speeds. The 18 × 5.5 tire-test speeds were 10, 40, 80, and 100 mph and the 49 × 17 tire-test speeds were 10, 40, 80, 120, and 160 mph.

Tire-time constant and dynamic yaw coefficient

The tire-time constant C_1 of Eq. (3) was determined for two vertical load conditions for each of the tires. The rolling tire-test rig used to obtain data for the yaw coefficient determination was also used for the determination of the time constant. The test rig was rotated about the pivot and allowed to reach steady-state condition at a fixed angle (approximately 6° for the 18 × 5.5 tire and 4° for the 49 × 17 tire) and then released. The ensuing angular motion was recorded and the amplitude ratios and frequencies were used in the determination of the time constant.

For a specified vertical loading F_z on the tire, a series of runs was made at various rolling speeds and trail lengths. Figure 6 presents the resulting amplitude ratios for one set of experimental data. The governing equations of motion of the test rig are given by Eqs. (2, 3, 5, and 6) which, along with the free oscillation condition and the use of an equivalent viscous damper expressed by

$$M_A = 0,\ M_B = -C_D\dot{\psi}$$

reduce to a linear, fourth-order system. The equivalent viscous damping C_D is estimated from friction data taken under static loading of the test rig and the empirical formula obtained for the analysis is

$$C_D = \frac{4M_B}{\pi\psi_0\omega} = \frac{1.59}{\psi_0\omega}\left[a\left(\frac{LF_z}{L_B}\right)^m L_B + b\left(\frac{L_B - L}{L_B}F_Z\right)^n\right]$$

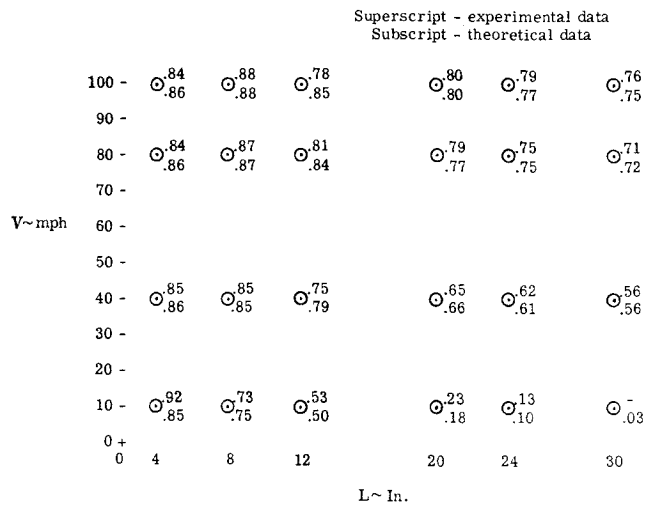

Fig. 6 Amplitude ratios from experimental and theoretical rolling tire data for 18 x 5.5 tire at 105 psi and 775-lb vertical load.

where
$a = 0.3925$, $b = 0.00586$, $m = 0.5$, $n = 1.2$, $\omega = [(L/C + \mu_1)/I]^{1/2}$, $\psi_0 = 0.07$ rad (average amplitude of oscillation) and L_B is the length to the load-support bearings shown in Fig. 3.

The solution of the linear equations of motion for the test-rig swivel angle ψ is found by classical methods and is represented functionally by

$$\psi \Rightarrow \psi(C_1, C, L, V)$$

where all the other tire parameters in the equation are determined from the test data. The amplitude ratio is defined as the ratio of neighboring peaks,

$$A = \psi_{n-1}/\psi_n \Rightarrow A(C_1, C, L, V)$$

The experimentally determined amplitude ratio at a point (L,V) is denoted by $A_e(L,V)$ and an error function is defined for each speed V as

$$e = \sum_L [A(C_1, C, L) - A_e(L)]^2 \Rightarrow e(C_1, C, V)$$

The problem of fitting the experimental data points with theoretical curves becomes one of choosing the values of C_1 and C which minimize the error e for each speed V. An example of the type of plots resulting from this method is shown in Fig. 7. Experimental and theoretical values of the frequency can also be compared to obtain a "square error" as done with the amplitude ratios. Both amplitude ratio error and frequency error were used to determine the values of C and C_1 given in Table 1. Although the frequency error depends considerably on the value of the yaw coefficient C, it is nearly

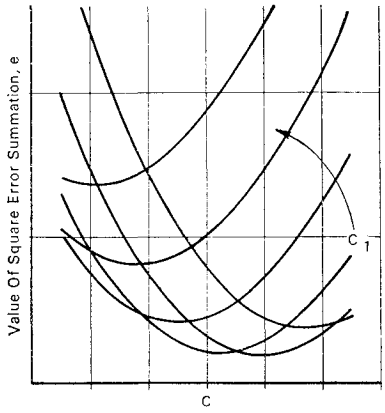

Fig. 7 Error study for C and C_1 determination.

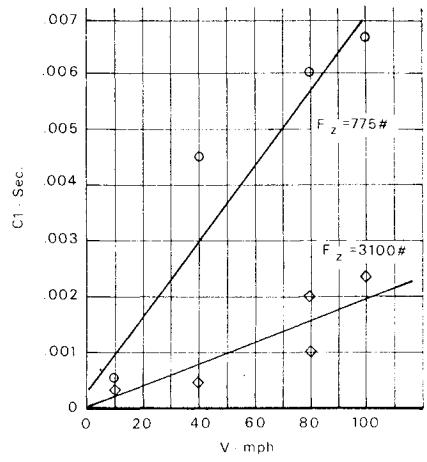

Fig. 8 Experimental values of C_1 for 18 x 5.5 tire at 105 psi.

independent of the value of C_1. The amplitude error is also more strongly dependent on the yaw coefficient than the time constant although the effect of time constant is significant. The value of C_1 was dependent upon V as indicated for one tire condition in Fig. 8 while the dynamic yaw coefficient is essentially independent of speed, as was also indicated in the steady-state tests. The values of the parameters k_1 and C_L required to determine the theoretical amplitudes were those obtained in the standing tire tests. The value of the torsional constant μ_1 did not significantly affect the determination of the values for C and C_1, probably because of the large trail lengths used in the testing. The value of μ_1 was taken as zero for the correlation. Figure 8 shows the results for C_1 obtained by this procedure for the 18 × 5.5 tire.

IV. Tire Parameter Effects on Landing-Gear Stability

The purpose of this section of the paper is to show, by way of examples, the importance of having accurate tire parameter data for prediction of landing-gear shimmy characteristics. It is beyond the scope of the present paper to give a complete presentation on the experimental programs and theoretical models used to obtain the shimmy-stability data presented here.

Types of Landing-Gear Shimmy

In analyzing the stability of a typical landing-gear system having a shimmy damper in series with the torsional elasticity of the strut, it is found that there are two types of shimmy motion. The occurrence of one or the other depends on the amount of damping available. For low damping, a type of shimmy occurs which involves rigid-body torsional motion of the landing gear restrained by the yawing motion of the tire. That is, the modal mass is essentially the moment of inertia of the swiveling parts of the landing gear about the swivel axis, and the effective spring rate is the tire dynamic-torsional spring rate plus the reciprocal of the tire-yaw coefficient multiplied by the perpendicular distance from the swivel axis to the line of action of the footprint lateral load. This first type of shimmy will be referred to as tire-yaw shimmy. For high-damping, tire-yaw shimmy becomes very stable and the structural modes of the gear can become unstable. One commonly occurring mode has essentially the same modal mass as the first mode; however, the spring rate is the torsional-spring rate of the landing gear with the damper locked. This type of shimmy will be referred to as structural-torsion shimmy.

Both types of shimmy motion are affected significantly by the tire parameters and parametric effects on both stability

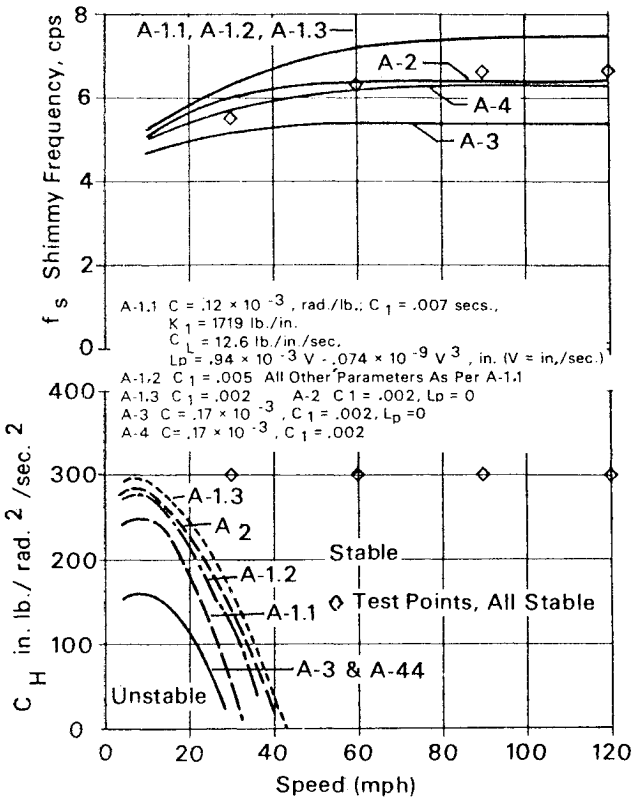

Fig. 9 Comparison of experimental shimmy frequencies and stability with predicted results and the effect of tire parameter variations on tire-yaw shimmy ("*A*" landing-gear configuration).

and frequency should be classified according to the type of shimmy. A considerable amount of confusion can result from general statements on the effect of both structural and tire parameters on shimmy without clarifying the type of shimmy for which the trends apply.

Tire Parameter Effects on Tire-Yaw Shimmy

The influence of C in the frequency of tire-yaw shimmy has been mentioned previously; however, C also has a significant effect on stability. Figure 9 shows theoretical stability and frequency plots for 6 combinations of tire parameters for a comparatively stable version of a test landing gear with 18 × 5.5, 14-ply, Type VII tires being used for experimental/theoretical correlation studies. Four experimental configurations of the landing gear were studied with *A–D* designations. All of the results shown plotted on Fig. 9 apply to the *A* configuration with the parameter set designated *A*-4 being approximately equal to the experimental parameters. It can be seen that the experimental shimmy frequencies agree quite closely with the theoretical predictions with parameter set *A*-4. The system is stable at $C_H = 300$ which agrees with all of the predictions with the various parameter sets.

Conditions *A*-1.3 and *A*-4 compare directly except for the value of C. The increase in C in condition *A*-4 results in a considerable increase in the stability. A similar trend is evident in comparing conditions *A*-3 and *A*-2.

The stabilizing influence of increasing C has been found to be true for tire-yaw shimmy over a wide range of system parameters. Analysis indicates it is somewhat equivalent to increasing the dimensionless damping of the system and reducing the frequency. Figure 9 also shows effects of varying C_1 (conditions *A*-1.1 through *A*-1.3). Here a stabilizing trend is evident with increasing C_1. This trend is not general. For certain combinations of parameters, increasing C_1 has the same effect as decreasing C in that it stiffens the tire from a yaw

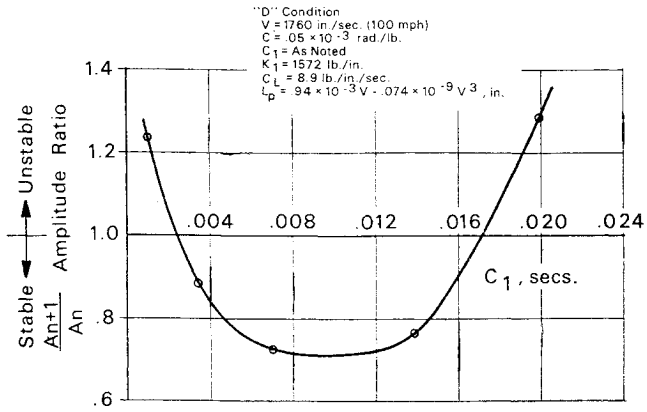

Fig. 10 Theoretical stability reversal with increasing C_1.

standpoint and decreases the stability of the system. For example, Fig. 10 shows a case where increasing C_1 is at first stabilizing but for sufficiently high C_1 further increases result in instability. In general if $2\pi f_s C_1 < 0.25$ increasing C_1 will be stabilizing, and if $2\pi f_s C_1 > 0.75$ increasing C_1 will be destabilizing for tire-yaw shimmy.

The effect of the dynamic tire torsional spring rate μ_1 was studied using the concept of "pneumatic trail" L_p. The relationship between L_p and μ_1 is given by

$$\mu_1\psi_t = (L_p/C)(\psi_t + C_1\dot{\psi}_t)$$

so that, for $2\pi f_s C_1 \ll 1.0$, $\mu_1 \simeq L_p/C$. Figure 9 shows a small destabilizing trend for increasing L_p (conditions *A*-1.3 and *A*-2). This is a general trend for all of the landing-gear systems studied with the degree of destabilization dependent upon the other tire parameters, particularly C. For smaller values of C, larger destabilization results from a given increase in L_p. For the tire-test machine, increases in L_p resulted in increased stability when the mechanical trail was in the stable region (large trail). Thus, for a large-trail landing-gear systems the influence of L_p could reverse. It can also be seen that L_p has a sizable influence on the shimmy frequency.

The stability of the analytical model of the landing-gear test system was not sensitive to changes in the lateral stiffness k_1 while in the tire-yaw shimmy mode. However, the analytical model of the tire parameter test machine showed a significant decrease in stability with decreasing k_1 as noted

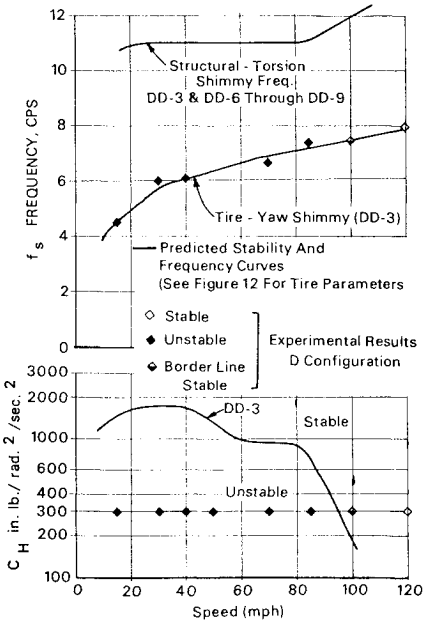

Fig. 11 Comparison of experimental shimmy frequencies and stability with predicted results.

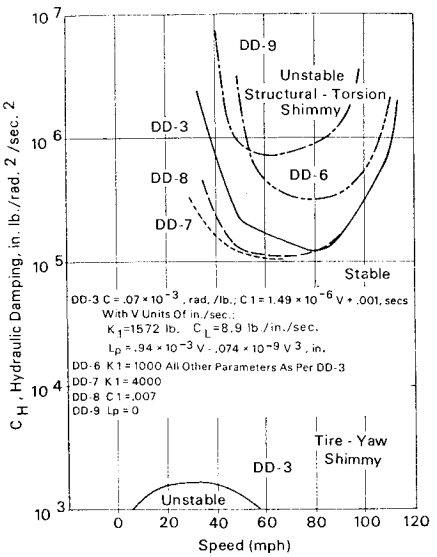

Fig. 12 Effect of tire parameter variations on structural-torsion shimmy.

by de Carbon in Ref. 5. The lateral damping C_L enters only as a stabilizing element, similar to the classical viscous damping mechanism. Surprisingly the lateral stiffness does not enter into the shimmy frequency in a significant manner.

The D configuration landing gear was a more unstable system than the A configuration and provides a somewhat more critical test of the correlation of the shimmy theory used here. The DD-3 parameter set, which will be discussed below in connection with the structural-torsion shimmy, is the best estimate of the experimental parameters for this gear system. A comparison of the experimental and theoretical results is given in Fig. 11. Although several factors contribute to the reduced stability of the D configuration, the main factor is the reduction in C. Note that C for condition DD-3 is 0.07×10^{-3} rad/lb whereas the quite stable A-4 configuration has a value of 0.17×10^{-3} rad/lb.

Tire-Parameter Effects on Structural-Torsion Shimmy

Figure 12 shows stability maps of the D configuration landing gear used in the experimental/theoretical correlation studies mentioned previously. The DD-3 parameter set corresponds approximately to the test system with DD-6 through DD-9 being theoretical parameter variations about this basic set.

Two regions of instability are shown in Fig. 12. The lower region of instability corresponds to the tire-yaw shimmy. The upper region corresponds to the structural-torsion shimmy, which is of concern in this section. The frequency of the structural-torsion shimmy is higher than the tire-yaw shimmy and is given in Fig. 11. For the tire-parameter variations discussed here, there was no significant variation in this frequency.

Although C variations are not shown in Fig. 12, it was found that by increasing C by a factor of 2.5 times the nominal value (case DD-3, $C = 0.07 \times 10^{-3}$) the boundary could be raised well above the $C_H = 10 \times 10^6$-in.-lb/rad^2/sec^2 upper limit of the figure. In short, it is a primary factor in determining the over-damped stability boundary.

Condition DD-8 shows the effect of increasing C_1. In contrast to the tire-yaw shimmy increased C_1 has a destabilizing effect for the structural-torsion shimmy. Whether this is a general trend or not is not known but this one example illustrates that a fairly accurate value of C_1 must be known to adequately predict the location of over-damped stability boundary.

Pneumatic trail or tire dynamic torsional spring rate has a strong influence on the stability boundary as shown by the profile for condition DD-9. Variations in k_1 are illustrated by conditions DD-3, DD-6, and DD-7, which correspond to k_1 values of 1572, 1000, and 4000 lb/in., respectively. A destabilizing trend with increased k_1 is evident which is the opposite effect of that found in tire-yaw shimmy.

V. Conclusions

1) The tire parameters $C, C_1, k_1 C_L$, and μ_1 (or equivalently L_p) provide an adequate representation of the tire for shimmy studies. The experimental methods presented here allow a direct determination of the first 4 parameters and bounds to be placed on μ_1. Although these parameters and the associated mathematical relationships are undoubtedly only approximations of the fundamental mechanics of a rolling pneumatic tire, they provide a highly useful analytical model.

2) The foregoing 5 tire parameters have significant effects on stability and/or frequency of both tire-yaw shimmy and structural-torsion shimmy. Accurate (or at least conservative) estimates of these parameters must be available to conduct a shimmy-stability study of a landing-gear system.

3) In an analytical study of the shimmy stability of a landing-gear system, it is recommended that ranges of values be considered on the tire parameters to account for items such as experimental error, variations in conditions at the footprint/ground surface interface, variation in tire properties with wear, and differences in the tire performance at shimmy frequencies vs the frequencies obtained in the tire tests.

4) Analytical predictions of stability and frequency of shimmy motions, using the tire mechanics equations presented here, show good correlation with experimental results.

References

[1] Von Schlippe, B., "Shimmying of a Pneumatic Wheel," TM-1365, Aug. 1954, NACA, pp. 125–147.

[2] Moreland, W. J., "The Story of Shimmy," *Journal of the Aeronautical Sciences*, Vol. 21, No. 12, Dec. 1954, pp. 793–808.

[3] Smiley, R. F. and Horne, W. B., "Mechanical Properties of Pneumatic Tires with Special Reference to Modern Aircraft Tires," TR R-64, 1960, NASA.

[4] Edman, J. L., "Experimental Study of Moreland's Theory of Shimmy," TR 56–197, July 1956, Wright Air Development Center, Wright-Patterson Air Force Base, Ohio.

[5] de Carbon, C. B., "Analytical Study of Shimmy of Airplane Wheels," TM-1337, Sept. 1952, NACA.